Proton emission cross sections of silicon isotopes

J. F. Dias, M. N. Martins, and E. Wolynec
Laboratório do Acelerador Linear, Instituto de Física da Universidade de São Paulo, São Paulo, Brazil
(Received 15 May 1990)

Measurements of the electrodisintegration cross sections, (e,p) and $(e,2p)$, and their corresponding electrodisintegration-plus-photodisintegration yields for ^{29}Si and ^{30}Si are presented. The experiment covers the range from 20 to 60 MeV electron incident energies. The experimental results were analyzed using $E1$ and $E2$ distorted-wave Born approximation virtual photon spectra for a finite nucleus in order to obtain the corresponding photodisintegration cross sections for both channels and isotopes. For ^{29}Si the integrated (γ,p) cross sections is 47% bigger than (γ,n) while for ^{30}Si they are of the same order of magnitude. For both isotopes the (γ,p) decay channel is dominantly $E1$. The $(\gamma,2p)$ channel is much smaller than the $(\gamma,2n)$ channel but the $E2$ contribution to this decay mode is of the same magnitude of the $E1$.

I. INTRODUCTION

Giant resonances are a common feature of all nuclei and have been extensively studied in the last 50 years. Yet there are few measurements of multiple charged particle emission in the decay process. Measurements carried out by Dodge *et al.*[1] for (e,p) and (e,α) cross sections in ^{90}Zr and ^{92}Zr, by Tamae *et al.*[2] for ^{90}Zr(e,α) and by Tanaka *et al.*[3] for ^{65}Cu(e,α) show a common feature. The corresponding photodisintegration cross sections, obtained through the virtual photon analysis, showed a nonresonant behavior, steadily increasing for increasing bombarding energies. Since it has been shown that DWBA virtual photon spectra for finite nuclei relate electrodisintegration and photodisintegration cross sections, showing good agreement between measured photodisintegration cross sections and those obtained from electrodisintegration measurements,[4,5] a failure of the virtual photon calculations to explain this strange behavior can be disregarded. Dodge *et al.*[1] pointed out that a possible explanation could be multiple alpha and proton emission, which would be interpreted as single events in all these experiments, since they detected, on line, the number of emitted charged particles. This explanation would imply that, as an example, the $2p$ decay channel should have a magnitude of about half of that of the one-proton decay channel. Furthermore, when the ^{65}Cu(e,α) cross section was measured by residual activity[6] the results differed from those of Ref. 3 and the obtained (γ,α) cross section showed a resonant behavior.

The lack of information, in the literature, on the decay of the giant resonance by $2p$ emission, motivated us to measure the (e,p) and $(e,2p)$ cross sections in ^{29}Si and ^{30}Si, to obtain their corresponding photodisintegration cross sections. These isotopes were chosen because they allow the measurements to be carried out by counting residual activity, thus distinguishing completely both decay channels. Apart from the interest in obtaining the relative magnitudes of the decay by one and two proton emission, it is important to study the fraction of the dipole strength carried out by proton emission.

The decay of the dipole giant resonance by neutron emission has already been measured for these isotopes[7] and it was found that this mode carries about half of one classical dipole sum. Since for silicon isotopes the Coulomb barrier is about 2.4 MeV for each proton emitted,[8] their (γ,p) cross sections are expected to be responsible for a non-negligible fraction of the giant resonance decay.

II. THE EXPERIMENT

The experiment was performed using the 60 MeV linear electron accelerator of the University of São Paulo. The electrodisintegration cross sections and the electrodisintegration-plus-photodisintegration yields were obtained by bombarding natural silicon targets and measuring, off line, their residual activity, counting the gamma rays emitted by their reaction products. The charge was obtained by using a Faráday cup for the electrodisintegration measurements and a ferrite monitor (calibrated to the Faraday cup) for the radiator-in measurements. Table I summarizes the reactions studied, their threshold energies, the energy and intensity of the detected gamma rays and the half-lives of the corresponding reaction products.

In order to allow enough time for the activity of reaction products to die out, measurements were carried out using four targets with 22 mg/cm^2 for electrodisintegration and three targets with 41 mg/cm^2 for electrodisintegration-plus-photodisintegration yields. For the activation of the electro plus photodisintegration yields a tantalum radiator with 275 mg/cm^2 was placed in the electron beam immediately ahead of the target.

Since the experiment was performed using natural silicon targets (92.2% ^{28}Si, 4.7% ^{29}Si, and 3.1% ^{30}Si),[9] the bombarding and counting times had to be adjusted in order to allow measurements of all reaction products by residual activity. An irradiation time of four hours was used for the reactions ^{30}Si$(e,2p)$ and ^{30}Si$(e+\gamma,2p)$ and the residual activity was counted for 24 hours. The other three reactions (see Table I), which yield half-lives of a few minutes, were simultaneously measured using bom-

TABLE I. Main features of the (γ,p) and $(\gamma,2p)$ reactions studied in this work. The threshold (Ref. 13) does not include the Coulomb barrier (Ref. 8) (about 2.4 MeV for each proton emitted). The other data were taken from Ref. 9.

Reaction	Decay product	E_γ (keV)	I_γ (%)	Half-life	Threshold (MeV)
^{29}Si$(e,p)^{28}$Al					
^{29}Si$(e+\gamma,p)^{28}$Al	$^{28}\text{Al}\xrightarrow{\beta^-}{}^{28}\text{Si}$	1778.7	100	2.24 min	12.3
^{29}Si$(e,2p)^{27}$Mg					
^{29}Si$(e+\gamma,2p)^{27}$Mg	$^{27}\text{Mg}\xrightarrow{\beta^-}{}^{27}\text{Al}$	843.8	73	9.46 min	21.9
^{30}Si$(e,p)^{29}$Al					
^{30}Si$(e+\gamma,p)^{29}$Al	$^{29}\text{Al}\xrightarrow{\beta^-}{}^{29}\text{Si}$	1273.2	89	6.56 min	13.5
^{30}Si$(e,2p)^{28}$Mg					
^{30}Si$(e+\gamma,2p)^{28}$Mg	$^{28}\text{Mg}\xrightarrow{\beta^-}{}^{28}\text{Al}$	30.6	95	20.93 h	24.0

barding times of 15 min. and counting times of about 20 min.

The gamma rays listed in Table I were detected using two high purity germanium detectors. One of them was used for the 30.6 keV gamma ray resulting from the decay products of the reactions ^{30}Si$(e,2p)$ and ^{30}Si$(e+\gamma,2p)$, which were studied using longer bombarding times, and the other for the 843.8, 1273.2, and 1778.7 keV gamma rays corresponding to the remaining studied reactions, which used shorter bombarding times. Both detector efficiencies were measured with calibrated standard gamma-ray sources, in the same fixed geometry used to detect gamma rays from the targets, thus avoiding the need to measure absolute efficiencies. In the counting geometry used the distance between target and detector was 4 cm. The data acquisition system consisted of an amplifier, and analog-to-digital converter and a computer-aided measurement and control system connected with a PDP 11/84 computer.

In Figs. 1 to 4 the results obtained for the electrodisintegration cross sections (solid circles) and for the electrodisintegration-plus-photodisintegration yields (solid squares) are presented. The error bars show the statistical uncertainties of the measurements when these are

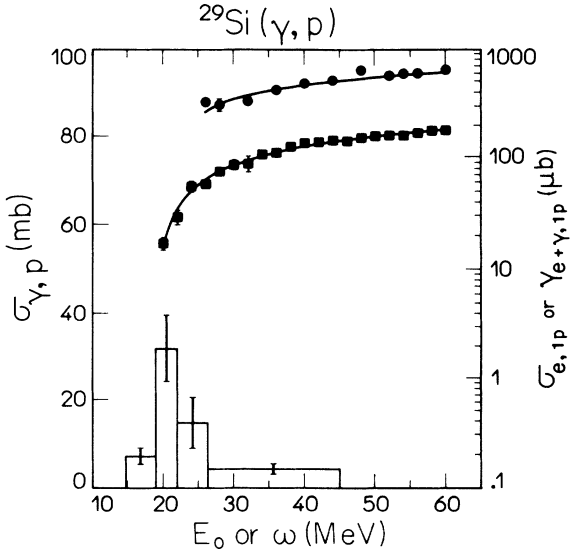

FIG. 1. The measured $\sigma_{e,p}(E_0)$ (solid squares) and yield $Y_{e+\gamma,p}(E_0)$ (solid circles) for ^{29}Si as a function of the incident electron energy E_0 (right-hand scale). The $Y_{e+\gamma,p}(E_0)$ was obtained when a 275 mg/cm^2 tantalum radiator was placed in the electron beam ahead of the target. The histogram represents the photodisintegration cross section, $\sigma_{\gamma,p}$ (left-hand scale). The smooth curves represent the best simultaneous fit to the electrodisintegration cross section [Eq. (1)] and the electrodisintegration-plus-photodisintegration yield [Eq. (2)] that originated the histogram (see text).

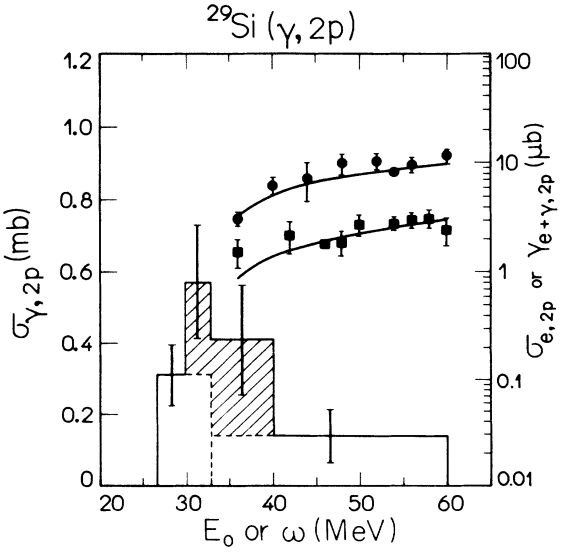

FIG. 2. $\sigma_{e,2p}$ for ^{29}Si. The dashed portion of the histogram represents the $E2$ contribution to the $(\gamma,2p)$ cross section. See caption of Fig. 1.

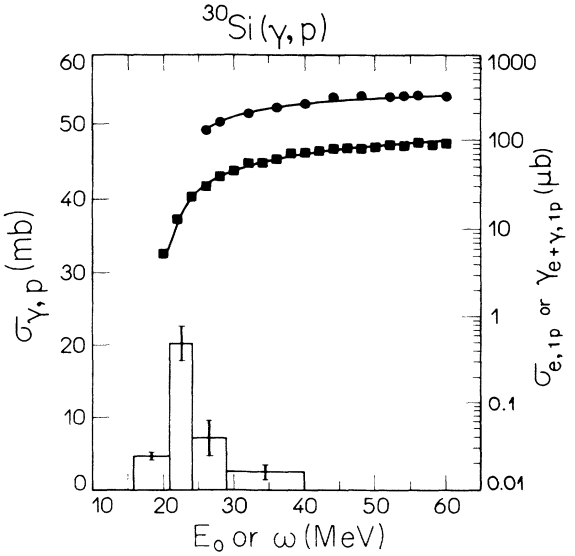

FIG. 3. $\sigma_{e,p}$ for ^{30}Si. See caption of Fig. 1.

larger than the points representing the measured cross sections or yields. The overall uncertainty in the absolute scale is about 20%.

II. DATA ANALYSIS AND RESULTS

The measured cross section and yields were analyzed using the virtual photon method which relates electrodisintegration and photodisintegration cross sections. According to this method, the relationship between the photodisintegration cross section $\sigma_{\gamma,x}$ and the measured electrodisintegration cross section $\sigma_{e,x}$ is

$$\sigma_{e,x}(E_c)=\int_0^{E_c}\sum_{\lambda l}\sigma_{\gamma,x}^{\lambda l}(E)N^{\lambda l}(E_c,E,Z,A)\frac{dE}{E} \quad (1)$$

where E_c is the electron kinetic energy; E is the photon energy; $N^{\lambda l}$ is the virtual photon spectrum calculated for a nucleus with atomic number Z and mass number A (Ref. 10) and λl is the multipolarity. The yield with the radiator in is

$$Y_{e+\gamma,x}(E_c)=\sigma_{e,x}(E_c-2\Delta)+N_r\int_0^{E_c-\Delta}\sigma_{\gamma,x}(E)N^{\mathrm{BR}}(E_c-\Delta,E,Z_r)\frac{dE}{E}, \quad (2)$$

where Δ is the electron energy loss in half the radiator thickness, N_r is the number of atoms/cm^2 of the radiator, and N^{BR} is the bremsstrahlung cross section for a radiator of atomic number Z_r.

Photodisintegration produced by bremsstrahlung in the target was calculated and found to be negligible when compared with the measured electrodisintegration cross sections or the electrodisintegration-plus-photodisintegration yields.

The virtual photon spectrum used[10] was calculated in the DWBA taking into account the size of the nucleus. The bremsstrahlung spectrum used is that calculated by Seltzer *et al.* and discussed in Ref. 11.

Figure 5 shows, for an electron incident energy of 30 MeV, the $E1$ and $E2$ virtual photon spectra calculated for ^{29}Si and the bremsstrahlung spectrum calculated for the Ta radiator used.

The photodisintegration cross sections were represented by histograms in Eqs. (1) and (2) and obtained by fitting simultaneously the electrodisintegration and electrodisintegration-plus-photodisintegration measurements, for each of the studied reactions, using the VIRLIB code.[12] It was assumed that only $E1$ and $E2$ multipoles contribute to the photonuclear processes in the energy region covered by the measurements. For the (γ,p) cross sections, in both isotopes, it was not possible to fit an $E2$

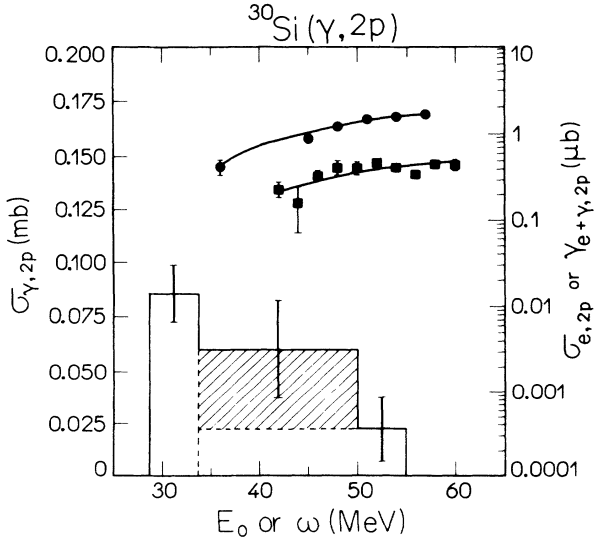

FIG. 4. $\sigma_{e,2p}$ for ^{30}Si. The dashed portion of the histogram represents the $E2$ contribution to the $(\gamma,2p)$ cross section. See caption of Fig. 1.

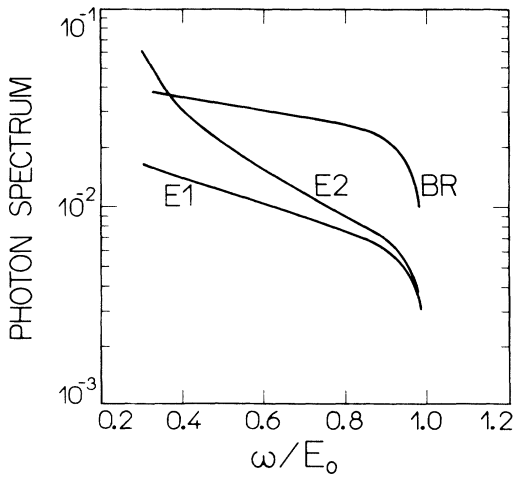

FIG. 5. The bremsstrahlung (BR) and the virtual ($E1$ and $E2$) photon spectra calculated for a kinetic electron energy of 30 MeV. The DWBA virtual photon spectra are those calculated by Onley *et al.* (Ref. 10), while the bremsstrahlung spectrum used is that calculated by Seltzer *et al.* (Ref. 11) (see text).

TABLE II. Integrated cross sections for (γ,p) and $(\gamma,2p)$ reactions on silicon isotopes.

Reaction	EL	χ^2 red.	Integrated cross section (MeV mb)	Energy range (MeV)	% of sum rule
^{29}Si(γ,p)	$E1$	1.03	269.3 (40.1)	14.7–45.0	70.0 (9.2)
^{29}Si$(\gamma,2p)$	$E1$	0.85	5.8 (2.1)	26.6–60.0	1.3 (0.5)
^{29}Si$(\gamma,2p)$	$E2$		2.5 (1.3)	30.0–40.0	15.3 (8.0)
^{30}Si(γ,p)	$E1$	0.76	150.8 (17.3)	15.9–40.0	33.7 (3.9)
^{30}Si$(\gamma,2p)$	$E1$	1.84	0.9 (0.4)	28.7–55.0	0.20 (0.09)
^{39}Si$(\gamma,2p)$	$E2$		0.6 (0.3)	33.5–50.0	2.6 (1.2)

component. The measurements were compatible with pure $E1$. For the $(\gamma,2p)$ cross sections the inclusion of an $E2$ component resulted in a much better fit than that obtained under the assumption of pure $E1$.

In Figs. 1 to 4, the histograms show the obtained photodisintegration cross sections for each reaction. The $E2$ contribution to the $(\gamma,2p)$ cross sections is shown by the dashed portions of the corresponding histograms. In these figures the full lines through the measured points show the results of the best simultaneous fits, which resulted in the presented histograms for each reaction. For all four reactions studied the compatibility of electrodisintegration and photodisintegration is excellent.

It has to be pointed out that the energy range of the fit was chosen in order to yield the best fit. Any other tentative fit to the $\sigma_{\gamma,p}$ or the $\sigma_{\gamma,2p}$ below or above the energies shown in Figs. 1 to 4 impoverished the quality of the fit, producing cross sections compatible with zero.

Table II summarizes the obtained photonuclear cross sections, presenting for each channel and multipole the integrated cross section and the corresponding percentage of the sum rule exhausted.

IV. DISCUSSION

Figures 6 and 7 show the photoproton cross sections $(\gamma,p+\gamma,2p)$ and the photoneutron cross sections $(\gamma,n+\gamma,pn)$ for ^{29}Si and $(\gamma,n+\gamma,pn+\gamma,2n)$ for ^{30}Si (Ref. 7). Table III shows the integrated cross sections for photoprotons and photoneutrons and the sum of these decay channels for both isotopes. The results show that the photoproton decay channel is as important as the photoneutron channel, being bigger than the latter for ^{29}Si and smaller for ^{30}Si. The sum of photoproton and photoneutron decays exhausts about one $E1$ sum.

Comparing Figs. 6 and 7 one sees that at the peak position ($\sim$20 MeV) (γ,p) is bigger than (γ,n) for ^{29}Si, while for ^{30}Si it is the reverse. The decay mechanism certainly depends on the number of available levels in the residual nucleus (density of final states). It happens that for ^{29}Si, at an excitation energy of 20 MeV, the residual nucleus reached through one-proton emission (^{28}Al) has about 180 levels[9] in the energy interval from ground state to 7.7 MeV, while the nucleus reached through one-neutron emission (^{28}Si) has only 50 levels in the energy interval from ground state to 11.5 MeV of excitation energy. For

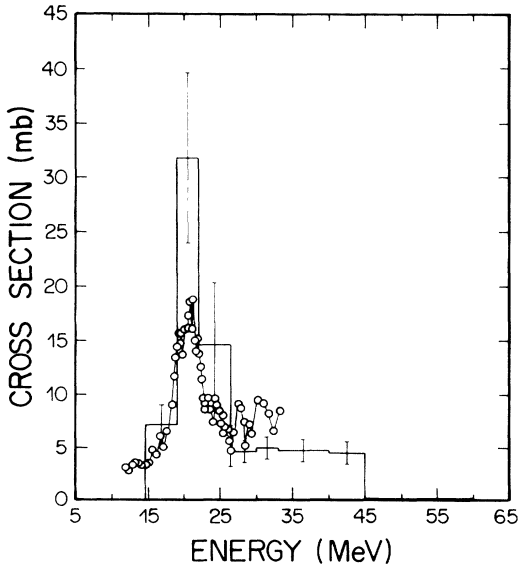

FIG. 6. The photoproton $(\gamma,p+\gamma,2p)$ cross section obtained in this work (histogram) and the photoneutron $(\gamma,n+\gamma,np)$ cross section (Ref. 7) (circles) for ^{29}Si.

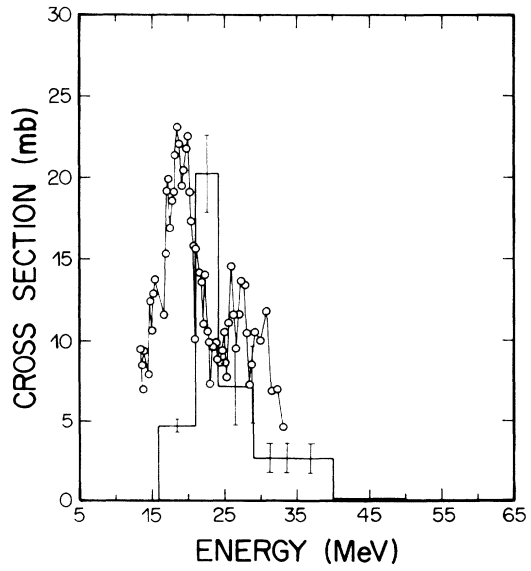

FIG. 7. The photoproton $(\gamma,p+\gamma,2p)$ cross section obtained in this work (histogram) and the photoneutron $(\gamma,n+\gamma,np)$ cross section (Ref. 7) (circles) for ^{30}Si.

TABLE III. Results obtained for $\sigma_{\gamma,xp}$ (this work) and $\sigma_{\gamma,xn}$ (Ref. 7) for silicon isotopes.

Reaction	Theshold (MeV)	Integrated cross section (MeV mb)	% of sum rule ($E1$)
^{29}Si(γ,p)	12.3	269.3	62.0
^{29}Si($\gamma,2p$)	21.9	5.8	1.3
^{29}Si(γ,n)	8.50	183.0	42.1
^{29}Si($\gamma,n+\gamma,np+\gamma,p+\gamma,2p$): 458.1 MeV mb			
^{30}Si(γ,p)	13.5	150.8	33.7
^{30}Si($\gamma,2p$)	24.0	0.9	0.2
^{30}Si(γ,n)	10.6	181.0	40.4
^{30}Si($\gamma,2n$)	19.1	67.0	15.0
^{30}Si($\gamma,n+\gamma,np+\gamma,2n+\gamma,p+\gamma,2p$): 399.7 MeV mb			

^{30}Si, at 20 MeV of excitation energy, the situation is reversed, since there are three times more levels in the residual nucleus that can be reached by neutron decay (^{29}Si) than in that reached by proton decay (^{29}Al).[9]

In both isotopes the $(\gamma,2p)$ cross section is much smaller than the (γ,p). The $(\gamma,2p)$ integrated cross section for ^{29}Si is five times bigger than that for ^{30}Si. For ^{30}Si the $(\gamma,2p)$ threshold is 4.9 MeV higher than the $(\gamma,2n)$, while for ^{29}Si the $(\gamma,2p)$ threshold is 3.8 MeV lower than the $(\gamma,2n)$. These differences in threshold may be responsible for the large differences in the $(\gamma,2p)$ integrated cross sections for ^{29}Si and ^{30}Si. Yet the $(\gamma,2p)$ cross sections in both isotopes present a common feature, they have an $E2$ component located in the energy range of the isovector $E2$ and they both exhaust a larger fraction of the $E2$ isovector sum than of the $E1$ sum.

While for both isotopes $E1$ dominates the one proton emission, $E2$ has an important participation in the two proton emission channel. Our results, however, cannot exclude a small $E2$ component in the one proton emission channel.

Both (γ,p) and $(\gamma,2p)$ cross sections present a resonant behavior and, because $(\gamma,2p)$ is much smaller than (γ,p), even in an experiment which would measure all protons and interpret all $2p$ events as two one-p events the resulting photoproton cross section would still have a resonant shape. This indicates that either the $(\gamma,2p)$ cross section is more important for Zr isotopes than it is for Si isotopes, or the results obtained in Refs. 1 and 2 have an explanation other than multiple particle emission.

ACKNOWLEDGMENTS

The authors would like to thank the Brazilian Agencies Fundação de Amparo a Pesquisa do Estado de São Paulo (FAPESP), Conselho Nacional de Desenvolvimento Científico e Tecnológico (CNPq), and Financiadora de Estudos e Projetos (FINEP) for supporting this work.

[1]W. R. Dodge, E. Hayward, M. N. Martins, and E. Wolynec, Phys. Rev. C **32**, 781 (1985).
[2]T. Tamae, T. Urano, M. Hirooka, and M. Sugawara, Phys. Rev. C **21**, 1758 (1980).
[3]T. Tanaka, Res. Rep. Lab. Sci., Tohoku Univ. **14**, 137 (1981).
[4]E. Wolynec, V. A. Serrão, and M. N. Martins, J. Phys. G Phys. **3**, 515 (1987).
[5]E. Wolynec, Nucl. Instrum. Methods A **280**, 358 (1989).
[6]M. N. Martins, E. Wolynec, and M. C. A. Campos, Phys. Rev. C **26**, 1936 (1982).
[7]S. S. Dietrich and B. L. Berman, *Atlas of Photoneutron Cross Sections Obtained with Monoenergetic Photons* (Academic, New York, 1981).
[8]J. B. Marion and F. C. Young, *Nuclear Reaction Analysis* (North-Holland, Amsterdam, 1968).
[9]C. M. Lederer and V. S. Shirley, *Table of Isotopes*, 7th ed. (Wiley, New York, 1978).
[10]D. S. Onley and F. Zamani Noor, Phys. Rev. C **33**, 1354 (1986).
[11]S. M. Seltzer and M. J. Berger, Nucl. Instrum. Methods B **12**, 95 (1985).
[12]VIRLIB is a modified version of code VIRLIN developed by R. Leicht. The changes were done by P. Gouffon and M. N. Martins.
[13]E. G. Fuller, H. M. Gerstenberg, and T. M. Collins, *Photonuclear Index*, Natl. Bur. Stand. Special Publication No. 332 (U.S. GPO, Washington, D.C., 1970).